Time-Resolved Fluorescence of *O*-Acetylserine Sulfhydrylase Catalytic Intermediates†

Sara Benci,*,‡ Silvia Vaccari,‡ Andrea Mozzarelli,*,§ and Paul F. Cook*,⊥

Institute of Physical Sciences and Istituto Nazionale per la Fisica della Materia, and Institute of Biochemical Sciences, University of Parma, 43100 Parma, Italy, and Department of Chemistry and Biochemistry, University of Oklahoma, 620 Parrington Oval, Norman, Oklahoma 73019

Received February 28, 1997; Revised Manuscript Received September 26, 1997⊗

ABSTRACT: The reaction of the substrate *O*-acetyl-L-serine (OAS) with the pyridoxal 5′-phosphate (PLP)-dependent enzyme *O*-acetylserine sulfhydrylase-A (OASS-A) proceeds via the transient formation of an external aldimine absorbing at 420 nm and a stable α-aminoacrylate intermediate absorbing at 330 and 465 nm. Stable external aldimine species are obtained by reaction of the enzyme with either the reaction product L-cysteine or the product analog L-serine. Static and time-resolved fluorescence emission properties of the coenzyme in the above catalytic intermediates have been used to directly probe the active site conformation at different stages of the catalytic pathway. Upon excitation at either 420 or 330 nm, the external aldimines with L-cysteine and L-serine exhibit a structured emission centered at 490 nm with a shoulder at 530 nm. Fluorescence decays upon excitation at 420 nm are best fitted using two components with lifetimes of 1.1 and 3.8 ns, with the fractional intensity of the slow component being 0.92 with L-cysteine and 0.75 with L-serine, respectively. The fast component, emitting at 530 nm, is attributed to a dipolar species formed in the excited state by proton dissociation, and the slow component, emitting at 490 nm, is attributed to a ketoenamine tautomer of the external aldimine. The slow component for external aldimine fluorescence decay is characterized by the same lifetime value as that of the internal aldimine with an increased fractional intensity, indicating that the distribution between the ketoenamine and the dipolar species is shifted toward the ketoenamine tautomer in the external aldimine, compared to the internal aldimine. Differences in equilibrium distribution of ketoenamine and enolimine tautomers can also account for differences in the emission properties of the external aldimines of L-cysteine and L-serine. The α-aminoacrylate species is characterized by a relatively weak emission. Upon excitation at 330 nm, the emission exhibits two bands centered at 420 and 540 nm, whereas upon excitation at 420 nm the emission bands are centered at 500 and 540 nm, and upon excitation at 465 nm, the main absorbance peak of the α-aminoacrylate species, the emission spectrum shows a band at 540 nm. The fluorescence decays, upon excitation at 330 nm, are best fitted using three components with lifetime values similar to those found for the internal aldimine, with the slow component predominating. Species-associated spectra, collected between 400 and 520 nm upon excitation at 350 nm, indicate the presence of a fast component overlapping the slow component on the blue side of the emission spectrum, as detected for the internal aldimine. When the excitation wavelength is 420 nm, there are only two components with the fast one predominating. A further increase in the fractional intensity of the fast component is observed upon excitation at 465 nm. The weak emission and the short lifetime of the emission excited at 465 nm indicate that this α-aminoacrylate tautomer interacts significantly with neighboring groups of the protein matrix and may be endowed with a higher mobility than the external aldimine.

O-Acetylserine sulfhydrylase is a dimeric pyridoxal 5′-phosphate[1] (PLP)-dependent enzyme that catalyzes the synthesis of L-cysteine *via* a *β*-replacement reaction from OAS and sulfide (Becker et al., 1969). The catalytic reaction, investigated by spectrophotometry (Cook et al., 1992; Schnackerz et al., 1995), luminescence (McClure and Cook, 1994; Strambini et al., 1996), ^{31}P NMR and circular dichroism spectroscopy (Schnackerz et al., 1995), initial velocity studies (Tai et al., 1993; Tai et al. , 1995), rapid-scanning and single-wavelength stopped-flow studies (Woehl et al., 1996), and kinetic deuterium isotope effects (Hwang et al., 1996) involves the sequential formation of several intermediates (Scheme 1): the internal aldimine, the *gem*-diamine, the external aldimine, and the α-aminoacrylate Schiff base. Tautomeric forms of some of these intermediates are suggested by the presence of multiple absorption bands (Cook et al., 1992; Schnackerz et al., 1995) and structured fluorescence (McClure and Cook, 1994) and phosphorescence emissions (Strambini et al., 1996).

† This work was supported by grants to P.F.C. from the National Science Foundation (MCB 9405020), a grant to S.B. and A.M. from the Italian National Research Council and MURST, and Grant No. CRG. 900519 from the North Atlantic Treaty Organization Scientific Affairs Division to P.F.C. and Dr. Klaus D. Schnackerz from the University of Würzburg, Germany.

‡ Institute of Physical Sciences and Istituto Nazionale per la Fisica della Materia.

§ Institute of Biochemical Sciences.

⊥ University of Oklahoma.

⊗ Abstract published in *Advance ACS Abstracts,* November 15, 1997.

[1] Abbreviations: PLP, pyridoxal 5′-phosphate; Hepes, 4-(2-hydroxyethyl)piperazine-1-ethanesulfonic acid; OAS, *O*-acetyl-L-serine; OASS-A, *O*-acetylserine sulfhydrylase, A-isozyme.

S0006-2960(97)00464-9 CCC: $14.00

Scheme 1: Catalytic Mechanism of OASS

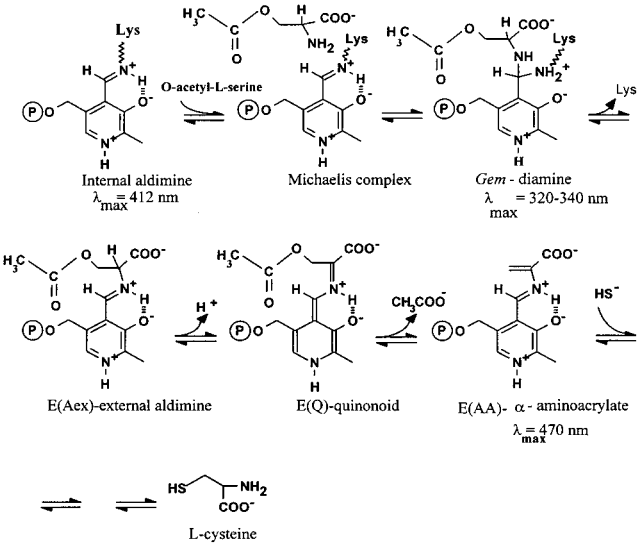

Formation of the external aldimine is likely accompanied by a transition from an open to a closed conformational state of the active site as signaled by changes in ^{31}P NMR and circular dichroism spectra (Schnackerz et al., 1995). Furthermore, the phosphorescence decay of W162, a residue 25 Å away from the active site, suggests that both the external aldimine and the α-aminoacrylate are endowed with a higher flexibility compared to the internal aldimine (Strambini et al., 1996; Burkhard et al., 1997).

In the present paper, the external Schiff bases, formed in the reaction of OASS with either L-serine or L-cysteine, and the α-aminoacrylate Schiff base, that accumulates when reacting OASS-A with the natural substrate OAS or with the substrate analog β-chloro-L-alanine in the absence of the nucleophilic substrate sulfide, have been characterized by static and time-resolved fluorescence. Previous fluorescence (McClure and Cook, 1994; Schnackerz et al., 1995) and phosphorescence emission studies (Strambini et al., 1996) were performed by excitation in the spectral region where aromatic amino acids absorb. In this study, PLP−OASS intermediates were investigated by excitation in the spectral range where PLP absorbs, thus directly probing the active site microenvironment and conformational events at different stages of catalysis.

MATERIALS AND METHODS

Enzymes. *O*-Acetylserine sulfhydrylase was prepared from wild type *Salmonella typhimurium* LT-2 according to the method of Hara (1990) as modified by Tai et al. (1993).

Chemicals. L-Serine, L-cysteine, *O*-acetyl-L-serine, β-chloro-L-alanine, and Hepes were the best commercial available quality and were used without further purification.

Buffers. Measurements were carried out in a solution containing 100 mM Na^+ Hepes, at either pH 7.0 or 9.0, 20 °C.

Absorption and Luminescence Spectra. Absorption spectra were collected on a Cary 219 interfaced to a computer and on a Cecil 3000 spectrophotometer (Milton Technical Center, Cambridge). Static fluorescence spectra were collected on a phase fluorometer (Model GREG 200, ISS Inc., Champaign, IL). The fluorescence intensity of the solvent was subtracted. Static fluorescence anisotropy was measured using the automatic procedure available on a Perkin-Elmer LS50B fluorometer. All cuvette holders were thermostated at 20 ± 0.5 °C. The concentration of OASS-A protomers was usually 13 μM.

Time-Resolved Fluorescence. Fluorescence decay was measured using the phase-modulation technique (Spencer & Weber, 1969; Gratton & Limkeman, 1983). The sample is excited with light of modulated intensity, and the phase shift and demodulation of the emitted light are determined as a function of the modulation frequency. Phase (τ_p) and modulation lifetimes (τ_m) are calculated according to eqs 1 and 2.

$$\tan P_m = \tau_p \quad (1)$$

$$M_m = [1 + (\omega\tau_m)^2]^{-1/2} \quad (2)$$

In eqs 1 and 2, P_m is the measured phase shift, M_m is the measured relative modulation ratio, and ω is the modulation angular frequency. The measured phase and modulation values were analyzed by assuming a sum of exponential decays. The resulting values were compared to the calculated values of phase and modulation (for any intensity decay) by using eqs 3 and 4

$$P_c = \tan^{-1}[S(\omega)/G(\omega)] \quad (3)$$

$$M_c^2 = S(\omega)^2 + G(\omega)^2 \quad (4)$$

In eqs 3 and 4, $S(\omega)$ and $G(\omega)$ have different expressions depending on the assumed model. For a sum of exponentials, $S(\omega)$ and $G(\omega)$ are given by eqs 5 and 6.

$$S(\omega) = \sum_i [f_i\omega\tau_i/(1 + \omega^2\tau_i^2)] \quad (5)$$

$$G(\omega) = \sum_i [f_i/(1 + \omega^2\tau_i^2)] \quad (6)$$

In eqs 5 and 6, the index i depends on the number of exponentials used for the fit, τ_i is the lifetime of the ith component, f_i is its fractional intensity, and thus $\sum f_i = 1$. The "goodness" of the fit is determined by the value of the reduced χ^2, defined in eq 7.

$$\chi^2 = \sum \{[(P_c - P_m)/\sigma_p]^2 + [(M_c - M_m)/\sigma_m]^2\}/(2n - F - 1) \quad (7)$$

In eq 7, n is the number of modulation frequencies and F is the number of free parameters, while σ_p and σ_m are the standard deviations of each phase and modulation measurement, respectively.

Variable-frequency phase and modulation data were measured on an ISS GREG 200 fluorometer using a reference solution of *p*-bis(2-phenoxazoyl)benzene (POPOP, $\tau = 1.35$ ns) or a glycogen scattering solution. Excitation was performed either using a 300 W xenon lamp with a Yobin Yvon monochromator with 16 nm band width or a dye laser synchronously pumped by a Nd-Yag laser (Coherent, Inc., Model 700). Emission bands were selected using cut-off filters.

Multiple-wavelength data were obtained using laser excitation at 350 nm and selecting nine distinct emission wavelengths with the monochromator (bandwidth, 8 nm) over the wavelength range 400−560 nm. To eliminate polarization artifacts in the determination of lifetimes, the

excitation beam was routinely polarized normal to the laboratory plane (0°) and the emission was collected at the magic angle (55°) (Spencer and Weber, 1970). Modulation frequency was varied continuously from 2−10 to 250 MHz. A set of 15 modulation frequencies was generally used in the frequency range most appropriate for the sample under investigation. Frequency-independent standard errors for phase and modulation were assumed to be 0.2° and 0.004, respectively. Decay data were fitted using a sum of exponential components, characterized by a lifetime, τ, and a fractional intensity, f, using software provided by ISS, Inc. Multiple-wavelength decay data were analyzed simultaneously at all emission wavelengths via the Global Unlimited software (Laboratory for Fluorescence Dynamics, University of Illinois, Urbana, IL) assuming fluorescence lifetimes independent of emission wavelength, while their associated fractional intensities were allowed to vary. The fitting procedure provides an estimate of the so-called "species associated spectra" (SAS) representing the emission spectrum of a given chemical species when excited-state reactions do not occur (Beechem & Gratton, 1988; Lakowicz, 1991). The multiple-wavelength decays were also analyzed separately at each wavelength assuming a model based on the sum of three unrelated exponentials. Samples were maintained at 20 ± 0.5 °C using a circulating water bath and a jacketed cell holder.

Fluorescence Anisotropy Decays. The rotational behavior of fluorescent molecules is investigated by detecting the differential polarized phase and modulation ratio between the perpendicular and parallel polarized components of the emission (Lakowicz, 1983; Weber, 1977). The above quantities are determined by rotating the emission polarizer upon excitation with polarized light using the instrumentation available at the Laboratory for Fluorescence Dynamics, Department of Physics, University of Illinois, Urbana, IL. The observed differential phase and modulation ratios depend upon the modulation frequency and the rotational rates of the sample, and thus, data were collected over the same wide frequency range used in fluorescence lifetime experiments. Fluorescence anisotropy decays are analyzed in a manner similar to fluorescence intensity decays. Parameters describing the anisotropy decay are obtained by a nonlinear least-squares analysis of the data using single and multiexponential models available from the Globals Unlimited software (Laboratory for Fluorescence Dynamics, Department of Physics, University of Illinois, Urbana, IL). The goodness of the fit is judged by a reduced χ^2, defined by an equation similar to that shown for intensity decays. For this procedure, it is assumed that the values of the fluorescence lifetimes and the fractional intensities have been determined in separate experiments. In the time domain the anisotropy data are analyzed in terms of multiple correlation times according to the following expression

$$r(t) = r_o \Sigma_i \alpha_i \, e^{-t/\tau_{cl}} \qquad (8)$$

where $r(t)$ is the anisotropy at time t, r_o is the limiting anisotropy, α_i is the preexponential factor of the ith rotational component, and τ_{cl} is the rotational correlation time of the ith component. The method to convert the above equation to the frequency domain and further details of the analysis of frequency domain data are given by Weber (1977) and Jameson and Hazlett (1991).

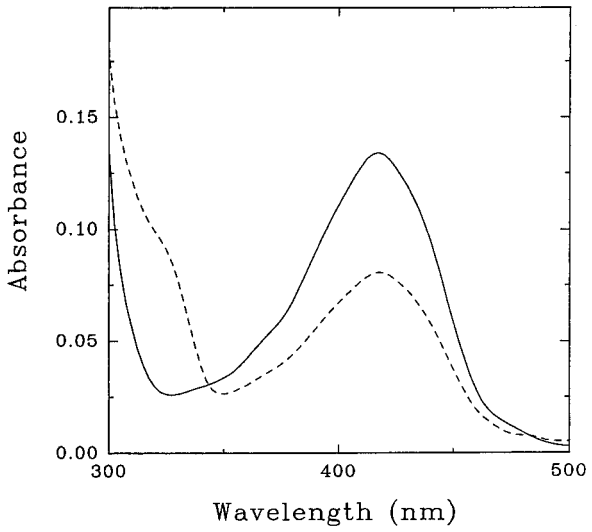

FIGURE 1: Absorption spectra of PLP−OASS (17.4 μM enzyme protomers) in the presence of 130 mM L-serine (dashed line) and 5 mM L-cysteine (solid line), 100 mM Hepes, pH 9.

RESULTS

Static and Time-Resolved Fluorescence of the External Aldimine of OASS-A with L-Cysteine and L-Serine. Binding of L-cysteine to OASS-A leads to a transient appearance of the α-aminoacrylate intermediate, Scheme 1, followed by the formation of an external Schiff base with L-lanthionine, a thioether formed by the Michael addition of the cysteine thiolate to C3 of the α-aminoacrylate intermediate (Woehl et al., 1996). The lanthionine external Schiff base exhibits an absorption band at 418 nm, Figure 1, slightly red shifted with respect to the band of the internal Schiff base (λ_{max}= 412 nm; Schnackerz et al., 1995). Fluorescence emission, upon excitation at 420 nm, is structured with a maximum at 490 nm and a shoulder at 530 nm, Figure 2a. Compared to the emission spectrum of the internal aldimine (S. Benci et al., unpublished results) the band at 490 nm in the external aldimine spectrum is enhanced and blue shifted by ∼3.5 nm, and the ratio of intensities at 490 and 530 nm is higher. Upon excitation at 330 nm, the emission intensities at 490 and 530 nm are lower than those observed with excitation at 420 nm but still significantly increased when compared to the internal aldimine, and the ratio of intensities at 490/530 is essentially constant. The emission band at 420 nm, which predominates in the emission of the internal aldimine (S. Benci et al., unpublished results), becomes a pronounced shoulder on the blue side of the band at 490 nm in the case of the external aldimine, Figure 2b.

Binding of the product analog L-serine gives an equilibrium mixture of external Schiff base tautomers absorbing at 422 and 330 nm, Figure 1. The species absorbing at 330 nm has been attributed to an enolimine tautomer of the external aldimine (Schnackerz et al., 1995). Fluorescence spectra, upon excitation at 420 nm, Figure 2a, show an intense band at 490 nm and a shoulder at 525 nm, similar to data obtained with L-cysteine. The 490 nm peak exhibits a lower intensity than that observed for the L-cysteine external aldimine, directly correlated to the decreased absorption intensity at 420 nm. Upon excitation at 330 nm, Figure 2b, the emission at 420 nm is a shoulder of the 490 nm band that exhibits the same intensity as in the L-cysteine enzyme derivative. Excitation spectra of L-serine external aldimine

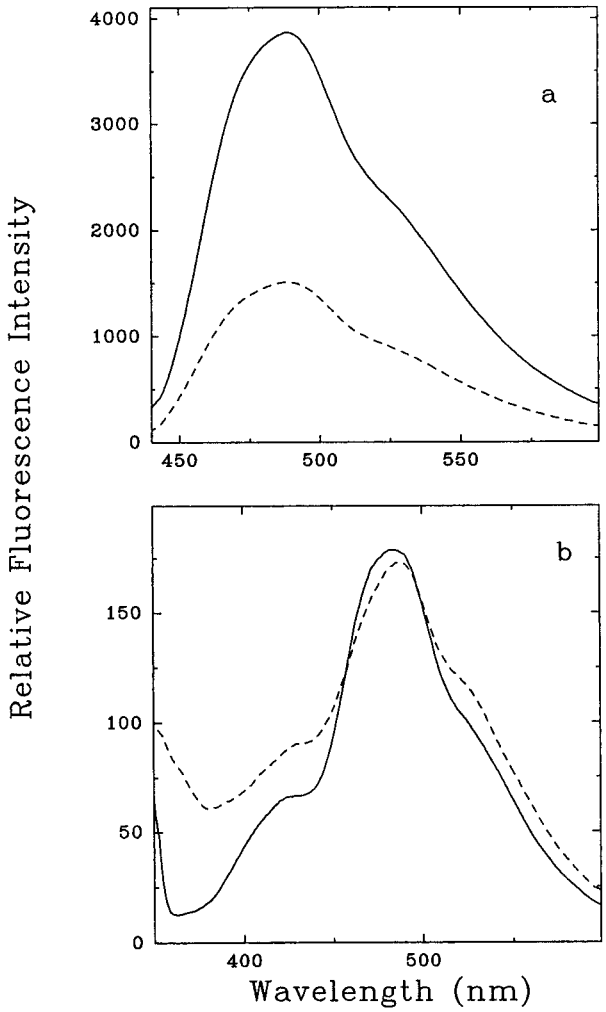

FIGURE 2: Fluorescence spectra of the external Schiff bases of OASS-A with L-cysteine and L-serine. OASS-A (17.4 μM enzyme protomers) in the presence of 130 mM L-serine (dashed line) and 5 mM L-cysteine (solid line), 100 mM Hepes, pH 9. Excitation was at 420 nm (a) and 330 nm (b).

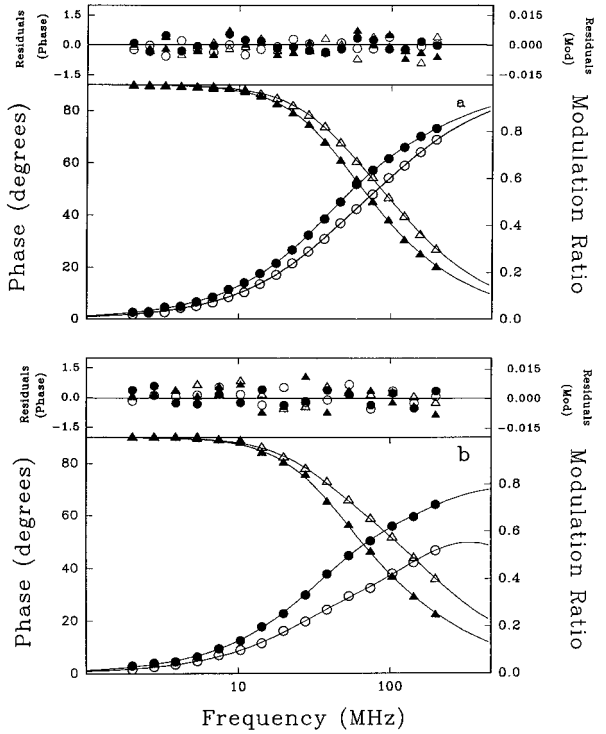

FIGURE 3: Time-resolved fluorescence of the external Schiff bases of OASS-A with L-serine and L-cysteine. Lifetime multifrequency phase (○, ●) and modulation (△, ▲) data for L-serine−OASS (open symbols) and L-cysteine−OASS (filled symbols) at 25 °C in 100 mM Na Hepes buffer, pH 9. The curves represent the least-squares best fits to two components. The upper panels show the distribution of residuals. (a) Samples were excited at 420 nm with a xenon lamp, and the emission was measured using a Oriel 52095 cutoff filter. The resolved fluorescence lifetimes for the L-serine−OASS complex are 3.74 ns ($f_2 = 0.75$) and 1.10 ns ($f_1 = 0.25$) ($\chi^2 = 1.38$) and for L-cysteine−OASS 3.85 ns ($f_2 = 0.92$) and 1.08 ns ($f_1 = 0.08$) ($\chi^2 = 1.20$), respectively. (b) Samples were excited at 330 nm, and the emission was measured using a Oriel 52053 cutoff filter. The resolved fluorescence lifetimes for L-serine−OASS complex are 4.10 ns ($f_2 = 0.57$) and 0.70 ns ($f_1 = 0.43$), ($\chi^2 = 2.45$) and for L-cysteine−OASS complex 4.03 ns ($f_2 = 0.85$) and 0.71 ns ($f_1 = 0.15$) ($\chi^2 = 2.31$), respectively.

have the same shape as those observed for the internal aldimine species with peaks at 330 and 290 nm when recorded at 420 nm and at 420 nm when recorded at 490 and 525 nm. However, they do reflect the reduced intensity of the 420 nm emission (data not shown).

Fluorescence decays of Schiff bases of OASS-A in the presence of L-cysteine and L-serine, upon excitation at 420 nm and emission at wavelengths higher than 470 nm, are best fitted using two components with lifetimes of 1.1 and 3.8 ns and a fractional intensity of the short component equal to 0.08 for L-cysteine and to 0.25 for L-serine (Table 1 and Figure 3a). Upon excitation at 330 nm and emission at wavelengths higher than 370 nm, the two lifetimes for the short component of L-cysteine and L-serine external Schiff bases are 0.71 and 0.70 ns and the fractional intensities are 0.15 and 0.43, respectively (Table 2 and Figure 3b). For comparison, lifetimes and fractional intensities of the internal aldimine are reported in Tables 1 and 2.

Static and Time-Resolved Fluorescence of the α-Aminoacrylate Schiff Base. The reaction of OAS or β-chloro-L-alanine with OASS-A leads to the appearance of two absorption bands centered at 465 and 330 nm, attributed to different tautomeric forms of the α-aminoacrylate Schiff base (Cook et al., 1992). The emission spectrum of the α-aminoacrylate species, upon excitation at 330 nm, exhibits two bands centered at 420 nm and 540 nm, Figure 4a, while excitation at 420 nm gives bands that are centered at 490 and 540 nm, Figure 4b. The emission spectrum, recorded upon excitation at 465 nm, indicates the presence of a single band at 540 nm, Figure 4c. Excitation spectra, collected at 420 nm (Figure 4a), 500 nm (Figure 4b), 530 nm (data not shown), and 555 nm (Figure 4c), indicate that the band at 420 nm is produced by excitation at 290 and 320 nm, the band at 500 nm is elicited by excitation at 290 nm, 320 nm, and maximally, at about 415 nm (these excitation bands are also responsible for the emission at 530 nm), and the band at 555 nm is elicited by excitation at about 410 nm with a shoulder at 465 nm. Emission and excitation spectra were also collected for β-chloro-L-alanine obtaining similar results (data not shown), as expected since the same α-aminoacrylate intermediate is produced in both cases (Tai et al., 1993).

Fluorescence decay data were collected in the presence of saturating concentrations of either OAS or β-chloro-L-alanine upon excitation at 330, 420, or 465 nm. Lifetime and fractional intensity values are summarized in Table 3. Three components are required to fit the decays upon excitation at 330 nm and recording the emission at wavelengths higher than 370 nm. Fluorescence decays were also

Table 1: Fluorescence Decay Parameters for the Internal and External Aldimine of OASS upon Excitation either at 412 or at 420 nm[a]

sample	pH	τ_1	τ_2	f_1	f_2	χ^2
internal aldimine−OASS	7	0.58 ± 0.02	3.77 ± 0.13	0.50 ± 0.01	0.50 ± 0.01	2.00
	9	0.65 ± 0.02	3.76 ± 0.13	0.52 ± 0.01	0.48 ± 0.01	3.54
L-cysteine−external aldimine−OASS	9	1.00 ± 0.04	3.85 ± 0.03	0.08 ± 0.01	0.92 ± 0.01	1.20
L-serine−external aldimine−OASS	9	1.18 ± 0.02	3.74 ± 0.04	0.25 ± 0.01	0.75 ± 0.01	1.38

[a] τ_1 and τ_2 are distinct lifetimes, expressed in ns, with fractional intensities f_1 and f_2, respectively. Excitation wavelength was 420 nm for L-cysteine or L-serine external aldimines and 412 nm for the internal aldimine. Emissions were recorded using a Oriel 52095 cutoff filter ($\lambda_{em} \geq 470$ nm). Values are the average of two to three measurements.

Table 2: Fluorescence Decay Parameters for the Internal Aldimine and the External Aldimine of OASS-A upon Excitation at 330 nm[a]

sample	pH	τ_1	τ_2	τ_3	f_1	f_2	f_3
internal aldimine−OASS[b]	7	0.43 ± 0.06	1.55 ± 0.06	6.97 ± 0.20	0.10 ± 0.01	0.32 ± 0.01	0.58 ± 0.01
	9	0.50 ± 0.05	1.60 ± 0.06	6.55 ± 0.20	0.18 ± 0.01	0.27 ± 0.01	0.54 ± 0.01
L-cys−external aldimine−OASS	9	0.71 ± 0.02	4.06 ± 0.05		0.15 ± 0.01	0.85 ± 0.01	
L-serine−external aldimine−OASS	9	0.70 ± 0.02	4.10 ± 0.10		0.43 ± 0.01	0.57 ± 0.01	

[a] τ_1, τ_2 and τ_3 are distinct lifetimes, expressed in ns, with fractional intensities f_1, f_2, and f_3 respectively. Excitation wavelength was 330 nm for all samples. Emissions were recorded using a Oriel 52053 cutoff filter ($\lambda_{em} \geq 370$ nm). Values are the average of two to three measurements.[b] Data from Benci et al. (unpublished results). Values of χ^2 are 4.9, 4.41, 2.31, and 2.45 from top to bottom.

Table 3: Fluorescence Decay Parameters for the α-Aminoacrylate Intermediate[a]

excitation and detection wavelength	lifetime and fractional intensity	
	plus OAS	plus β-chloroalanine
exc 330 nm	τ_1 0.17 ± 0.04	τ_1 0.58 ± 0.03
em ≥ 370 nm	τ_2 1.30 ± 0.06	τ_2 1.46 ± 0.30
	τ_3 6.60 ± 0.20	τ_3 6.80 ± 0.20
	f_1 0.12 ± 0.01	f_1 0.19 ± 0.01
	f_2 0.29 ± 0.01	f_2 0.10 ± 0.01
	f_3 0.59 ± 0.01	f_3 0.71 ± 0.01
exc 420 nm	τ_1 0.24 ± 0.02	τ_1 0.48 ± 0.02
em ≥ 470 nm	τ_2 2.20 ± 0.20	τ_2 3.75 ± 0.40
	f_1 0.64 ± 0.01	f_1 0.70 ± 0.01
	f_2 0.36 ± 0.01	f_2 0.30 ± 0.01
exc 420 nm	τ_1 0.24 ± 0.02	τ_1 0.36 ± 0.02
em ≥ 520 nm	τ_2 2.14 ± 0.32	τ_2 3.49 ± 0.32
	f_1 0.71 ± 0.02	f_1 0.72 ± 0.02
	f_2 0.29 ± 0.02	f_2 0.28 ± 0.02
exc 465 nm	τ_1 0.10 ± 0.02	τ_1 0.10 ± 0.03
em ≥ 520 nm	τ_2 2.14 ± 0.50	τ_2 2.12 ± 0.50
	f_1 0.91 ± 0.02	f_1 0.89 ± 0.02
	f_2 0.09 ± 0.02	f_2 0.11 ± 0.02

[a] The selected emissions were obtained using Oriel 52053, 52095, and 52102 cutoff filters, respectively. τ are the distinct lifetimes expressed in ns and f the fractional intensities and χ^2, the reduced chi-square, ranges from 2.5 to 5.8 for all measurements. Values are the average of two to three measurements.

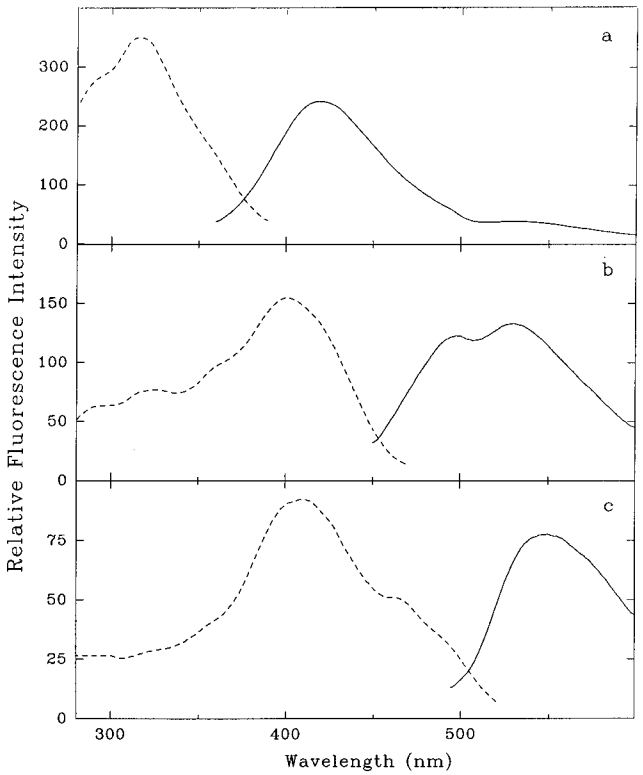

FIGURE 4: Emission and excitation spectra of α-aminoacrylate−OASS intermediate. Spectra of OASS (38.3 M enzyme protomers) after addition of 5 mM OAS in 100 mM Hepes, pH 7 were recorded at different excitation and emission wavelengths. (a) Fluorescence spectrum (solid line) for excitation at 330 nm and excitation spectrum (dashed line) recording the emission at 420 nm. (b) Fluorescence spectrum (solid line) for excitation at 420 nm and excitation spectrum (dashed line) recording the emission at 500 nm. (c) Fluorescence spectrum (solid line) for excitation at 465 nm and excitation spectrum (dashed line) recording the emission at 555 nm.

recorded varying the emission wavelength between 400 and 520 nm. The fluorescence decays were simultaneously fitted by linking the lifetime values, Figure 5. At the blue side of the emission band the fractional intensity of the slow component increases as a function of wavelength, as in the case with the internal aldimine (S. Benci et al., unpublished results), indicating the presence of a fast component with a contribution that decreases from 400 to 450 nm. The large contribution of the 420 nm band to the emission spectrum, Figure 4a, indicates that the slow component predominates over the entire spectral range. Overall, lifetime values are not very different from those of the internal aldimine species, Table 2. Excitation at 420 nm, recorded at wavelengths higher than 520 nm, gives an emission that contains two components. The short-lived component has a τ_1 of 0.24 ns and a fractional intensity of 0.71, while the long-lived one exhibits a lifetime value of 2.14 ns and f_2 of 0.29. When the excitation wavelength is 465 nm and the emission is collected at wavelengths higher than 550 nm, the long-lived component exhibits the same lifetime value but with a reduced f_2 value, while the short component is characterized by a lifetime of 0.10 ns and a fractional intensity of 0.91. A similar behavior is obtained in the presence of β-chloro-L-alanine, as expected.

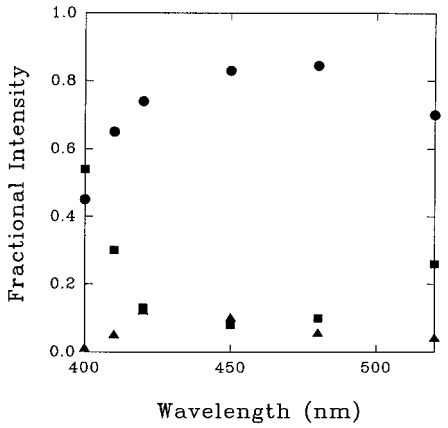

FIGURE 5: Species associated spectra of α-aminoacrylate−OASS Schiff base. Species associates spectra were determined upon excitation at 330 nm using a dye laser for a solution containing OASS, 5 mM OAS, 100 mM Hepes, pH 7 at 25 °C. Emissions were recorded at selected wavelengths between 400 and 520 nm. Decays were simultaneously fitted assuming three lifetimes with values independent of wavelength. Spectra correspond to the following lifetimes: $\tau_3 = 6.40$ ns (●); $\tau_2 = 1.35$ ns (■); $\tau_1 = 0.14$ ns (▲). Total reduced $\chi^2 = 6.50$.

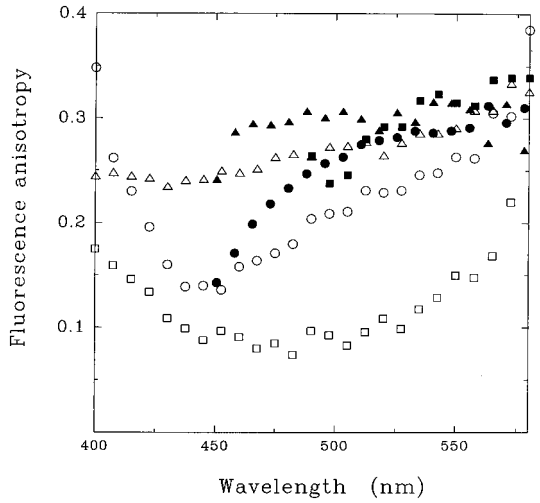

FIGURE 6: Steady-state fluorescence anisotropy spectra of the internal aldimine−OASS, L-serine−external aldimine−OASS, and the α-aminoacrylate−OASS, at pH 7.0 and 9.0. Fluorescence anisotropy of a solution containing OASS (14 μM enzyme protomers), 100 mM Hepes, 20 °C, was determined by measuring fluorescence polarization spectra with excitation light polarized either parallel or perpendicular to the emission light. Internal aldimine−OASS, pH 7 (identical curves were obtained at pH 9, data not shown), excitation at 350 nm (open circles); excitation at 412 nm (filled circles). L-Serine−external aldimine−OASS (130 mM L-serine), pH 9, excitation 350 nm (open triangles), excitation at 420 nm (filled triangles). α-aminoacrylate−OASS (5 mM OAS), pH 7, excitation at 350 nm (open squares), excitation at 465 nm (filled squares).

Static and Time-Dependent Fluorescence Anisotropy. Fluorescence anisotropy spectra of the internal, L-serine external, and the α-aminoacrylate Schiff bases of OASS-A were measured upon excitation at wavelengths corresponding to the absorption peaks, Figure 6. The fluorescence anisotropy value for the internal Schiff base upon excitation at 350 or 412 nm, and for the α-aminoacrylate Schiff base upon excitation at 350 or 465 nm, varies between 0.1 and 0.3 as a function of wavelength. A more constant value (0.25−0.31) is observed for the fluorescence anisotropy of the external aldimine upon excitation at either 350 or 420 nm. Similar values of fluorescence anisotropy (0.24) have been reported by Kwon et al. (1994) for a pyridoxylalbumin sample excited at 320 nm.

Measurements of the decay of fluorescence anisotropy of the internal aldimine of OASS-A in the presence and absence of acetate and of the α-aminoacrylate species were carried out upon laser excitation at 350 nm and have been analyzed using a number of different models. The χ^2 minimization indicates that the best fit is obtained using a two-component exponential decay model. For the internal aldimine, in the absence and presence of acetate, the observed rates are associated with an identical slow rotational correlation time ($\tau_{cl} = 21$ ns), but different anisotropy amplitudes, $f = 0.55$ and $f = 0.90$, and also different fast rotational correlation times of 2.42 and 0.58 ns, respectively. The limiting value for r_o is 0.315. Similar values have been reported by Sassaroli et al. (1986) for PLP bound to apo-hemoglobin upon excitation at 330 nm, 25 °C. In the case of the α-aminoacrylate intermediate, the best fit is obtained using two much smaller rotational correlation times ($\tau_1 = 1.6$ ns and $\tau_2 = 0.5$ ns) with a lower limiting value of r_o (0.2).

DISCUSSION

In this paper, PLP emissions have been characterized under conditions in which the coenzyme interaction with the active site of OASS-A is modified as a result of the reaction pathway, that is formation of intermediates such as the external aldimine and the α-aminoacrylate Schiff base. Information is obtained on conformational events that take place in the active site during catalysis.

Interpretation of Spectral Data Obtained for External Schiff Bases. Formation of the L-cysteine external Schiff base of OASS-A results in a red shift in the absorbance maximum of the internal aldimine absorption band from 412 to 418 nm (Schnackerz et al., 1995) and an enhancement in the 490 nm emission upon excitation at either 420 or 330 nm. A similar behavior is observed in the presence of L-serine. Enhancement of the 490 nm emission has also been detected upon excitation of native OASS-A in the presence of L-cysteine at 298 nm (McClure and Cook, 1994; Schnackerz et al., 1995). The 490 nm emission has been attributed to a ketoenamine tautomer (Arrio-Dupont, 1970, 1971; Cambron et al., 1996). The above findings thus suggest that in the external aldimine species either the ketoenamine tautomer is favored over the enolimine tautomer compared to the internal aldimine or a conformational change has occurred in the transition from the internal to the external aldimine leading to a more stable excited state of the ketoenamine tautomer. The analysis of fluorescence decays upon excitation at 420 nm clearly indicates that the long lifetime component, associated with the 490 nm emission, exhibits the same value for the internal and external aldimine ($\tau = 3.8$ ns) but with a higher fractional intensity for the external aldimine ($f = 0.92$ for L-cysteine; $f = 0.75$ for L-serine) compared to the internal aldimine ($f = 0.50$), suggesting that the former hypothesis is correct. A different behavior was observed for the tryptophan synthase $\alpha_2\beta_2$ complex, where an increase in the lifetime of the ketoenamine tautomer of the external aldimine (5.3 ns) is observed when compared to the internal aldimine ($\tau = 2.9$ ns), indicating a modification of the excited state stability of the ketoenamine tautomer of the external aldimine in the $\alpha_2\beta_2$ complex (Vaccari et al., 1996, 1997).

Scheme 2: Photophysical Model for PLP Decay in PLP−Schiff Bases upon 330 nm Excitation[a]

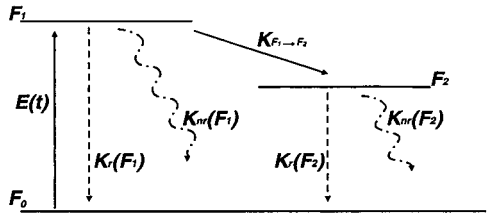

[a] $\tau_{F1} = [k_r(F_1) + k_{nr}(F_1)]^{-1}$ is the lifetime of the F_1 molecules that do not participate in the transfer reaction, $\tau_{(F1+F2)} = [k_r(F_1) + k_{nr}(F_1) + k_{F1\rightarrow F2}]^{-1}$ is the lifetime of the fluorophore in the presence of an excited state reaction, and $\tau_{F2} = [k_r(F_2) + k_{nr}(F_2)]^{-1}$ is the lifetime of the F_2 species. k_r and k_{nr} are rate constants for radiative and radiationless decay, respectively, and $k_{F1\rightarrow F2}$ is the $F_1 \rightarrow F_2$ transfer rate constant.

The decreased emission intensity at 490 nm for OASS-A in the presence of L-serine compared to L-cysteine, upon excitation at 420 nm, parallels the decreased absorption at 420 nm. The decreased absorbance likely results from a shift in the ketoenamine−enol imine equilibrium favoring the latter species and thus decreasing the concentration of the more strongly emitting ketoenamine (Schnackerz et al., 1995). The equal emission intensity for L-cysteine and L-serine external aldimines at 420 nm upon excitation at 330 nm is likely the result of the decreased amount of the ketoenamine tautomer formed in the excited state in the latter species (Benci et al., unpublished results). In fact, the observation of the same lifetime for both external aldimines indicates that the conformation of these intermediates is the same regardless of which amino acid is used.

The excitation of the external aldimines at 330 nm leads to a weak emission at 412 nm that overlaps the absorption band of the ketoenamine, whereas most of the absorbed energy is emitted at 490 nm with a shoulder at 530 nm. As in the case of the internal aldimine (S. Benci et al., unpublished results), the emission at 412 nm signals the presence of a weakly absorbing species at 330 nm, likely the enolimine tautomer of the Schiff base, which is particularly stable in an apolar environment (Arrio-Dupont, 1970; Kallen et al., 1985; Schnackerz et al., 1995). The emission and excitation spectra and the fluorescence decay data for the 490 and 530 nm bands are similar and indicate that, as for the internal aldimine, these two emissions are not directly and significantly excited at 330 nm. Therefore, the emission of the ketoenamine species is very likely due to ketoenamine formed in the excited state from enolimine via a proton-transfer reaction.

The proposed proton-transfer reaction that occurs in the excited state can be described by a two-state reaction scheme (Scheme 2). The F_1 species would be comprised of the tautomeric forms of the PLP Schiff base excited mainly at 330 nm, while the F_2 species would be comprised of (a) tautomeric form(s) of the PLP Schiff base emitting mainly at 490 and 530 nm. The proposed model for an irreversible process involving the interaction of two excited states assumes only that the F_1 state is populated upon absorption of light at 330 nm $E(t)$. On the basis of the experimental results obtained for the internal aldimine, the emission on the blue side of the spectrum is assumed to be due largely to the decay of the population of the F_1 state, characterized by the long lifetime value of 6.8 ns. The lifetime of the fluorophores in the F_1 state that contribute to the excited state reaction is decreased to 1.6 ns. According to eq 9

$$1/\tau_{F1+F2} = 1/\tau_{F1} + 1/\tau_{F1\rightarrow F2} \quad (9)$$

the rate constant for proton transfer, $k_{F1\rightarrow F2}$, is estimated as 4.8×10^{10} s^{-1}, giving a value of 2.1 ns for $\tau_{F1\rightarrow F2}$. The rate of interconversion from the enolimine to the ketoenamine tautomers is higher in the external aldimines than in the internal aldimine, and therefore, the longer lifetime is not detectable and the intermediate lifetime is shortened, becoming indistinguishable from the short one (Table 2).

In general, fluorescence lifetimes increase as the temperature is decreased or solvent viscosity is increased (Lakowicz, 1983). This effect can be attributed to a decreased frequency of collisions that lead to deactivation. Thus, the presence of predominant components with a long lifetime in the fluorescence decay of the PLP-external aldimine suggests a stabilization of the fluorophore environment in this species compared to the internal aldimine.

The emission of the external aldimine, as well as the internal aldimine (Benci et al., unpublished results), upon excitation at 330 or 420 nm, shows the presence of a shoulder at 530 nm. In PLP model compounds, the 530 nm emission has been attributed to a dipolar Schiff base formed by imine proton dissociation in the excited state (Arrio-Dupont, 1971; Cambron et al., 1996). Moreover, the different absorption and emission spectra of the L-cysteine and L-serine external aldimines and the different lifetime fractional intensities are consistent with a smaller contribution to the emission by the dipolar form emitting at 530 nm in the L-cysteine external aldimine, thus suggesting a more stable L-cysteine ketoenamine species. The more stable ketoenamine species is in agreement with ^{31}P NMR studies that indicate a tighter interaction of the 5′-phosphate of PLP in the case of the L-cysteine external aldimine, when compared to the L-serine external aldimine and the internal aldimine (Schnackerz et al., 1995).

Interpretation of Spectral Data Obtained for the α-Aminoacrylate Schiff Base. In the reaction of OASS-A with OAS or β-chloro-L-alanine, an external aldimine species is transiently formed and is rapidly converted to the α-aminoacrylate Schiff base by releasing acetate and a proton, as signaled by the appearance of bands at 470 nm (Cook and Wedding, 1976; Cook et al., 1992; Schnackerz et al., 1979; Woehl et al., 1996). A second band, centered at 330 nm, is also observed and has been attributed to a tautomeric form of the α-aminoacrylate. In the case of tryptophan synthase, the α-aminoacrylate species absorbs exclusively at 350 nm with a broad band extending to 500 nm (Miles, 1979; Drewe and Dunn, 1985). In the presence of nucleophilic substrates, like sulfide in the case OASS-A or indole in the case of the β-subunit of tryptophan synthase, the reactive α-aminoacrylate intermediate is irreversibly transformed to cysteine or tryptophan, respectively. For the α-aminoacrylate Schiff base of OASS-A, the broad and weak emission band at 540 nm, obtained upon excitation at 465 nm, is attributed to a short-lived species ($\tau \approx 0.10$ ns, $f = 0.9$) overlapping with a species with longer lifetime ($\tau = 2.14$ ns). For the α-aminoacrylate species of tryptophan synthase, weak emissions at 480 and 560 nm with short lifetime (0.4 ns) are also found upon excitation at 350 nm (Vaccari et al., 1996). The weak fluorescence intensity and the short lifetime of the α-aminoacrylate intermediate indicate that this species interacts significantly with neighboring groups of the protein matrix. Such interactions with the protein matrix, together

with an increased exposure to solvent, contribute to fluorescence quenching and might correlate with the high chemical reactivity of the α-aminoacrylate species. Tryptophan phosphorescence decays at 0 °C indicate an increased flexibility of the α-aminoacrylate intermediate with respect to the internal aldimine and a similar flexibility with respect to the external aldimine (Strambini et al., 1996). However, ^{31}P NMR spectra of the internal aldimine and α-aminoacrylate OASS are identical, suggesting a very similar rigidity in the 5′-phosphate binding pocket.

Assignment of the long-lived component of the emission decay in the presence of OAS, detected upon excitation at 465 nm, is difficult. On the basis of its lifetime value, the long-lived component might be assigned to the external aldimine of OAS or to some other species that is excited mainly at lower wavelengths. In fact, when excited at 420 nm, the emission spectrum indicates the presence of at least two species emitting at 500 and 540 nm (Figure 4b) with a slightly increased contribution of the long wavelength band for *β*-chloroalanine. Fluorescence decays can be attributed to two components with lifetimes and fractional intensities in agreement with the presence of two equally intense emission bands. An even more complex behavior is observed upon excitation of the α-aminoacrylate intermediate at 330 nm. The emission band is asymmetric with a maximum at 420 nm and a shoulder at 540 nm. The time-resolved decay of the emission can be accounted for by three components (Table 3), characterized by lifetimes and fractional intensities close to those of the internal aldimine. The longer lifetime value ($\tau = 6.6$ ns and $\tau = 7.6$ ns for OAS and *β*-chloroalanine, respectively) is characterized by a higher fractional intensity ($f = 0.59$ and $f = 0.71$, respectively) and corresponds to the decay of the 420 nm emission. The other lifetimes can be associated with the emission at higher wavelengths, as demonstrated for the internal aldimine species (Benci et al., unpublished results). In fact, an emission band at 490 nm is likely to be present as signaled by the asymmetry of the main band. The decreased intensity of the 490 nm band might be due to the presence of the 465 nm absorption band. Results of fluorescence decay data, recording the emission at wavelengths from 400 to 520 nm (Figure 5), suggest that, as for the internal aldimine species, two emissions are observed when exciting at 330 nm, with two different lifetime values corresponding to two excited states very close in energy. Also in this case, upon excitation at 330 nm, formation of tautomers and/or dipolar species emitting at lower energies is likely to occur in the excited state. Excitation spectra indicate that emissions at 500 nm are associated to bands at about 412 and 330 nm, while the excitation for the internal aldimine show that the emission at 500 nm can be excited at 420 and 280 nm (Benci et al., unpublished results). Moreover, the emission at 420 nm is excited at 330 nm, and the emission of the α-aminoacrylate observed at 550 nm is excited at either 465, 420, or 330 nm. These findings indicate that in the presence of substrates the number and the characteristics of the fluorescent PLP species changes leading to complex emission spectra and decays.

Fluorescence Polarization. When different species are present, or multiple electronic transitions for the same species occur, the polarization may be dependent on the excitation wavelength (Feofilov, 1961; Lakowicz, 1983). Indeed, upon excitation at 350 nm, the presence of at least three tautomeric forms with overlapping emission spectra and an excited state process between enolimine and ketoenamine tautomers would explain both the low anisotropy values and the observed changes as a function of emission wavelength.

Polarized emission spectra of the internal aldimine species, recorded at different excitation wavelengths, are in agreement with the observed heterogeneity of the fluorescence decay data being associated with the emission of distinct tautomeric species. Unfortunately, with the available resolution in this complex system, it is not possible to associate an observed correlation time to a rotational mode of a particular fluorescent species. However, the experimentally determined rotational correlation time of 21 ns is consistent with the value expected for the global motion of a protein with molecular weight of 69 000 Da. In fact, the theoretical estimate of the rotational correlation time for OASS at 25 °C gives $\Phi_c = 25.6$ ns, calculated using the Stokes−Einstein relationship for rotation of a spherical body according to the following expression

$$\Phi_c = M(\upsilon + \delta)\eta/RT \qquad (10)$$

where R is the gas constant, T is the absolute temperature, υ is the specific volume of the protein (∼0.733 cm^3/g), δ is the hydration state of the protein (∼0.3 cm^3/g), η is the viscosity of water (8.9×10^{-3} P at 25 °C), and M is the molecular mass. A rotational correlation time of 20 and 26.4 ns has been reported for bovine serum albumin (MW 64 000) at 25 °C (Lakowicz, 1983; Greenaway and Ledbetter, 1987), and a value of 20.8 ns has been reported for the dimer of chymotrypsin (MW 45 200; Lakowicz, 1983). A value of 38 ns has also been observed for the fluorescent probe I-EDANS tightly bound to pyridoxal kinase (Churchich and Wu, 1981). The rotational correlation time is strongly dependent on temperature, ranging from 45 ns at 44 °C to 4.4 ns at 5 °C for human serum albumin (Lakowicz, 1983). The value we report is in good agreement with those reported for other globular proteins of similar molecular weight. The lower rotational correlation time accounts for a low fraction of the total anisotropy and is presumably due to either the local motion of the probe within the active site or a structural motion of the environment around PLP. Results indicate that PLP in the internal aldimine of OASS-A is rigidly bound, in agreement with previous spectral data (Schnackerz et al., 1995). The decreased fractional intensity of the short rotational correlation time in the presence of acetate indicates a further reduction in flexibility at the coenzyme binding site.

The high anisotropy value for the L-serine external Schiff base and the low dependence of fluorescence anisotropy on emission and excitation wavelengths are consistent with the decreased complexity of the emission spectrum and fluorescence decay upon excitation at 330 or 420 nm, compared to the internal Schiff base. Therefore, the high anisotropy value, almost independent of the excitation wavelength, indicates that PLP in the external Schiff base is in a constrained environment and rotates with the protein.

In the case of the α-aminoacrylate species, the fluorescence anisotropy values strongly depend on excitation wavelengths. Upon excitation at 465 nm, the fluorescence anisotropy is close to that of the internal and external Schiff bases, thus indicating that the species absorbing at 465 nm rigidly rotates with the protein. On the other hand, the low value of

fluorescence anisotropy upon excitation at 350 nm could be explained by either rotational freedom and/or an increased transfer of excitation between fluorescent species. The anisotropy correlation times in the nanosecond and subnanosecond range detected for the α-aminoacrylate Schiff base of OASS-A might be due to motions of the probe. The short rotational correlation times and the low steady-state anisotropy of the α-aminoacrylate intermediate are indeed characteristic of a species with increased rotational freedom of the fluorescent probes.

Finally, OASS has been crystallized (Rao et al., 1993) and the three-dimensional structure of the internal aldimine determined (Burkhard et al., 1997). Preliminary functional studies of the crystalline enzyme (A. Mozzarelli and P. F. Cook, unpublished results) indicate that the external aldimines of L-cysteine and L-serine and the α-aminoacrylate intermediate can be formed in the crystal, thus opening the way to their structural determination. The structural investigations will add further information to that accumulated by fluorescence and phosphorescence studies on the relationship between protein dynamics and catalytic reaction.

CONCLUSIONS

On the basis of the present data, a sequence of conformational changes seems to accompany the formation of the external aldimine and α-aminoacrylate intermediates. Specifically, the internal aldimine is a heterogeneous mixture of compact and flexible tautomers. Binding of substrate to form the external aldimine stabilizes the tautomeric species characterized by a more compact structure, somewhat similar to the structure generated in the internal aldimine when the product acetate is bound. The structure generated might be favorable for the correct alignment of active site residues involved in the β-elimination reaction. When the α-aminoacrylate Schiff base is formed, the active site becomes more mobile, in agreement with the necessity to allow release of the nucleophilic product and add the nucleophilic substrate. Some of the same conformational events can be observed in the closely homologous β-subunit of the enzyme tryptophan synthase (Strambini et al., 1992a,b; Vaccari et al., 1997), thus suggesting common protein matrix adaptability to ligand binding and catalysis for these proteins.

ACKNOWLEDGMENT

The experiments with dye laser excitation were performed by one of us (S.V.) at the Laboratory for Fluorescence Dynamics (LFD) at the University of Illinois at Urbana−Champaign (UIUC). LFD is supported jointly by the Division of Research Resources of the National Institutes of Health (RR03155-01). We are indebted to Prof. Enrico Gratton and Dr. T. Hazlett, Department of Physics, University of Illinois at Urbana, for assistance in these measurements. We are also grateful to Prof. Klaus Schnackerz, University of Wurzburg, Germany, for critical reading of the manuscript.

REFERENCES

Arrio-Dupont, M. (1970) *Photochem. Photobiol. 12*, 297−315.
Arrio-Dupont, M. (1971) *Biochem. Biophys. Res. Commun. 44*, 653−659.
Becker, M. A., Kredich, N. M., & Tomkins, G. M. (1969) *J. Biol. Chem. 244*, 2418−2427.
Beechem, J. M., & Gratton, E. (1988) *SPIE 909*, 70−81.
Burkhard, P., Rao, G. S. J., Hohenester, E., Cook, P. F., & Jansonius, J. N. (1997) (manuscript in preparation).
Cambron, G., Sevilla, J. M., Pineda, T., & Blazquez, M. (1996) *J. Fluor. 6*, 1−6.
Churchich, J. E., & Wu, C. (1981) *J. Biol. Chem. 256*, 780−784.
Cook, P. F., & Wedding, R. T. (1976) *J. Biol. Chem. 251*, 2023−2029.
Cook, P. F., Hara, S., Nalabolu, S., & Schnackerz, K. D. (1992) *Biochemistry 31*, 2298−2303.
Drewe, W. F., & Dunn, M. F. (1985) *Biochemistry 24*, 3977−3987.
Feovilov, P. P. (1961) *The physical basis of polarized emission*, Consultants Bureau, New York.
Gratton, E., & Limkeman, M. (1983) *Biophys. J. 44*, 315−324.
Greenaway, F. T., & Ledbetter, J. W. (1987) *Biophys. Chem. 28*, 265−271.
Hara, S., Payne, M. A., Schnackerz, K. D., & Cook, P. F. (1990) *Protein Expression Purif. 1*, 70−90.
Hwang, C.-C., Woehl, E. U., Dunn, M. F., & Cook, P. F. (1996) *Biochemistry 35*, 6358−6365.
Jameson, D. M., & Hazlett, T. L. (1991) in *Biophysical and Biochemical Aspects of Fluorescence Spectroscopy* (Dewey, G., Ed.) pp 105−133, Plenum Press, New York.
Kallen, R. G., Korpela, T., Martell, A. E., Matsushima, Y., Metzler, C. M., Metzler, D. E., Morozov, Y. V., Ralston, I. M., Savin, F. A., Torchinsky, Y. M., & Ueno, H. (1985) in *Transaminases* (Christen, P., & Metzler, D. E., Eds.) pp 37−108, Wiley, New York.
Kwon, O. S., Blazquez, M. & Churchich, J. E. (1994) *Eur. J. Biochem. 219*, 807−812.
Lakowicz, J. R. (1983) *Principles of Fluorescence Spectroscopy*, Plenum Press, New York.
Lakowicz, J. R. (1991) *Topics in Fluorescence Spectroscopy*, Vol. 2, pp 241−277, Plenum Press, New York.
Lakowicz, J. R., Cherek, H., Kusba, J. , Gryczynski, I., & Johnson, M. L. (1993) *J. Fluor. 3*, 103−115.
McClure, G. D., & Cook, P. F. (1994) *Biochemistry 33*, 1674−1683.
Miles, E. W. (1979) *Adv. Enz. Relat. Areas Mol. Biol. 49*, 127−186.
Rao, G. S. J., Mottonen J., Goldsmith, E. J., & Cook, P. F. (1993) *J. Mol. Biol. 231*, 1130−1132.
Sassaroli, M., Kowalczyk, J., & Bucci, E. (1986) *Arch. Biochem. Biophys. 251*, 624−628.
Schnackerz, K. D., Ehrlich, J. H., Giesemann, W., & Reed, T. A. (1979) *Biochemistry 18*, 3557−3563.
Schnackerz, K. D., Tai, C.-H., Simmons, J. W. Jacobson, T. M., Jagannatha Rao, G. S. & Cook, P. F. (1995) *Biochemistry 34*, 12152−12160.
Spencer, R. D., & Weber, G. (1969) *Ann. N. Y. Acad. Sci. 158*, 361−376.
Spencer, R. D., & Weber, G. (1970) *J. Chem. Phys. 52*, 1654−1663.
Strambini, G. B., Cioni, P., Peracchi, A., & Mozzarelli, A. (1992a) *Biochemistry 31*, 7527−7534.
Strambini, G. B., Cioni, P., Peracchi, A., & Mozzarelli, A. (1992b) *Biochemistry 31*, 7535−7542.
Strambini, G. B., Cioni, P & Cook, P. F. (1996) *Biochemistry 35*, 8392−8400.
Tai, C.-H., Nalabolu, S. R., Jacobson, T. M., Minter, D. E., & Cook, P. F. (1993) *Biochemistry 32*, 6433−6442.
Tai, C.-H., Nalabolu, S. R., Simmons, W. J., III, Jacobson, T. M., & Cook, P. F. (1995) *Biochemistry 34*, 12311−12325.
Vaccari, S., Benci, S., Peracchi, A., & Mozzarelli, A. (1996) *Biophys. Chem. 61*, 9−22.
Vaccari, S., Benci, S., Peracchi, A., & Mozzarelli, A. (1997) *J. Fluor. 7*, 135S−137S.
Weber, G. (1977) *J. Chem. Phys. 66*, 4081−4091.
Woehl, E. U., Tai, C-H, Dunn, M. F., & Cook, P. F. (1996) *Biochemistry 35*, 4776−4783.

BI970464I